Forecasting reservoir inflows using remotely sensed precipitation estimates: A pilot study for the River Naryn, Kyrgyzstan

Journal:	*Hydrological Sciences Journal*
Manuscript ID:	HSJ-2014-0082.R1
Manuscript Type:	Original Article
Date Submitted by the Author:	n/a
Complete List of Authors:	Dixon, Samuel; Loughborough University, Geography Wilby, Robert; Loughborough University,
Keywords:	TRMM, Flow forecast, Toktogul reservoir, Central Asia, Regression model

SCHOLARONE™
Manuscripts

1 **Forecasting reservoir inflows using**

2 **remotely sensed precipitation**

3 **estimates: A pilot study for the River**

4 **Naryn, Kyrgyzstan.**

5

6 Samuel G. Dixon and Robert L. Wilby

7 Department of Geography, Loughborough University, Loughborough, Leicestershire, LE11 3TU, UK

8

9

10

11

14

15 Main body words: 5813

16

17 18 October 2014

18

19

20 Corresponding author:

21 Robert L Wilby

22 Department of Geography

23 Loughborough University

24 Loughborough

25 Leicestershire

26 LE11 3TU

27

28 Email: r.l.wilby@lboro.ac.uk

29 Tel: +44 1509 223093

30

31 **Abstract**

32 This study explores the feasibility of applying remotely sensed precipitation

33 estimates (in this case from the Tropical Rainfall Measuring Mission [TRMM]) for

34 forecasting inflows to the strategically important Toktogul reservoir in the Naryn

35 basin, Kyrgyzstan. Correlations between observed precipitation at Naryn and 0.5°

36 TRMM totals is weaker for daily (r=0.25) than monthly (r=0.93) totals, but the Naryn

37 gauge is representative of monthly TRMM precipitation estimates across ~60% of

38 the basin. We evaluate predictability of monthly inflows given TRMM estimates, air

39 temperature, and antecedent flows. Regression model skill was superior to the Zero

40 Order Forecast (mean flow) for lead times up to three months, and had lower errors

41 in estimated peaks. Over 80% of the variance in monthly inflows is explained with

42 three month lead, and up to 65% for summer half-year average. The analysis also

43 reveals zones that are delivering highest predictability and hence candidate areas for

44 surface network expansion.

45

46 **Key words**

1 Introduction

Early river flow forecasting systems relied on accurate ground based measurements of precipitation at meteorological stations – a basic input requirement that is still difficult to achieve in data sparse and/or physically remote regions (Artan et al., 2007). Partial information on precipitation variation in space and time continues to limit the development of flow forecasts for infrastructure operation and hazard warning (Bitew et al., 2012; Kekete et al., 2004). Even where data exist, absence of treaties for information sharing can hinder modelling and management of extreme events in transboundary situations (Hossain, 2007).

Remotely sensed, near real-time precipitation estimates have the potential to address these shortcomings (Hughes, 2006; Su et al., 2008; Collischonn and Pante, 2011) and may offer particular advantages for strengthening flow forecasts for large, transboundary river basins (Balthrop and Hossain, 2010). These capabilities have attracted growing attention from researchers and national agencies alike, with short-term flood forecasting models utilising passive microwave data for both precipitation and discharge estimation (e.g., Hopson and Webster, 2010; Hirpa et al., 2013).

The purpose of this paper is twofold. First, we assess the accuracy of a remotely sensed precipitation product for a strategically significant river basin in Central Asia. Second, we investigate the potential for river flow forecasting based on remotely sensed precipitation, surface temperature and gauged discharge, over monthly to seasonal horizons. We evaluate the data and forecasting techniques using flows in the Syr Darya, Kyrgyzstan upstream of the Toktogul reservoir. This system was chosen because of the importance of the basin as a 'water tower' for sustaining livelihoods downstream (Immerzeel et al., 2010). In addition to socio-economic challenges the region also faces a range of geophysical and meteorological hazards. Earthquakes and landslides are common in the Tien Shan, with most of the population of Kyrgyzstan living in areas of high or very high seismic hazard (UNDP, 2012). The primary meteorological hazard in the Syr Darya is flooding, which can be exacerbated by reservoir operations (UNDP, 2012).

The following section provides more background to the pilot study region and data. Section 3 describes the methods used to evaluate satellite products, and to build

80 statistical forecast models of reservoir inflows, drawing on input data from different

81 scales and locations within the basin. Section 4 presents the results of these

82 analyses, and Section 5 offers interpretations of model skill based on the

83 hydrometeorological processes within the basin. Finally, section 6 briefly considers

84 the transferability of the approach beyond the Naryn-Syr Darya cascade and offers

85 suggestions for further research.

86

2 Study area and data

88 The Naryn basin is located in the Central Tien Shan mountain range of Kyrgyzstan,

89 the headwaters of the Syr Darya River (**Figure 1**). The Syr Darya is one of two major

90 rivers (along with the Amu Darya) that supplies water to the Central Asian Republics.

91 The basin area of the Naryn is 55,944 km^2 with an elevation range of more than

92 4,000 m including major mountain belts such as the Kyrgyz Range in the north,

93 Talas Ala Toosu and Fergana ranges in the southwest (Kriegel et al., 2013). The

94 Naryn is fed by a major tributary below Song Kol Lake which runs during the melt

95 season (April to September). Land cover is mainly grass and shrub, with pastoral

96 farming on mountain sides, and some arable crop and hay production in valleys

97 sustained by irrigation.

98 The Tien Shan mountain range has a continental climate with the main source of

99 moisture originating from the Atlantic Ocean (Aizen et al., 1995a). Several weather

100 systems meet over the region, including westerly air streams, the Siberian

101 anticyclone and south/south-westerly cyclonic circulations (Aizen et al., 1995a; 2001).

102 The mountains prevent penetration of moisture into central areas resulting in low

103 winter precipitation, with maximum totals typically occurring in June and July (Aizen

104 et al., 1995a; 1996). Orographic factors produce a general decrease in precipitation

105 and temperature along a north-west to south-east gradient (Sorg et al., 2012,

106 Karaseva et al., 2012). Temperatures vary from 30°C in the western valleys in

107 summer to -25 °C in the glacierised regions in winter, but values as low as -50 °C

108 have been recorded in the Ak-Say valley. Snow depth is dependent upon aspect

109 relative to the western air masses, and an average melt season of ~70 days has

110 been observed in northern parts of the region (Aizen et al., 1995a; b).

4

111   The Naryn River has mean annual discharge of 13.8 km^3 with more than 50% of the

112   flow originating from snow and glacier melt (Savoskul et al., 2003). The Syr Darya

113   has been extensively managed to re-allocate water to satisfy the needs of countries

114   through which it flows (Kyrgyzstan, Uzbekistan, Tajikistan and Kazakhstan). Six

115   large and several smaller reservoirs were built along the Syr Darya by the Soviet

116   Union, providing a total storage capacity of ~35 km^3 (Savoskul et al., 2003). These

117   reservoirs have contributed to a management system described as one of the most

118   complicated in the world (Raskin et al., 1992).

119   Water diversions from the Syr Darya have contributed to the Aral Sea losing two-

120   thirds volume since 1957 (UNEP, 2008). Contention also surrounds the differing

121   interests of Kyrgyzstan to release water for hydropower generation during the winter,

122   versus downstream needs of Uzbekistan and Kazakhstan for irrigation in summer

123   (Karaev, 2005). During the Soviet era such energy-water trade-offs were managed

124   centrally (Hodgson, 2010); post-independence Kyrgyzstan has increased the volume

125   of water released from Toktogul during winter months for hydropower to reduce the

126   risk of black outs (Umaraliev, 2012). Attempts have been made to resolve these

127   competing interests (Kraak, 2012a) with operation of Toktogul reservoir central to

128   such discussions due to the immense storage capacity (19.5 km^3) and position of the

129   impoundment within the system (**Figure 1**).

130

2.1 Remotely sensed precipitation

132   UNDP (2012) concluded that as well as greater regional cooperation, there is also a

133   need to strengthen monitoring and modelling capacity in the region. Remotely

134   sensed precipitation data offer a means of filling these gaps. Several satellite

135   precipitation products are available including: the Tropical Rainfall Measuring

136   Mission (TRMM) and its successor the Global Precipitation Measurement (GPM)

137   Core Observatory (launched February 2014)[1]; Precipitation Estimation from

138   Remotely Sensed Information using Artificial Neural Networks (PERSIANN); and

139   NOAA Center for Satellite Applications and Research (STAR).

---

[1] http://www.nasa.gov/content/goddard/nasa-rainfall-satellite-out-of-fuel-but-continues-to-provide-data/#.VDLDG_nueuJ

140 This study demonstrates proof of concept using the TRMM Multi-satellite

141 Precipitation Analysis (TMPA) but our approach is applicable to other sources of

142 remotely sensed data. The TRMM product was constructed in four stages (NASA,

143 2011). First, microwave precipitation estimates are calibrated and combined; second,

144 infrared precipitation estimates are created with the aid of the calibrated microwave

145 precipitation estimates; third, microwave and infrared estimates are combined; and

146 fourth, rain gauge data are incorporated into the final estimate. Microwave

147 precipitation estimates are collected by multiple satellites (TRMM, DMSP, Aqua and

148 NOAA) which cover the area between 50°N and 50°S. Infrared data are collected by

149 the TRMM satellite and provides high temporal and spatial coverage. Rain gauge

150 data used in TRMM were obtained from Global Precipitation Climatology Centre

151 (GPCC) and the Climate Assessment and Monitoring System (CAMS) (Huffman et

152 al., 2007; Huffman and Bolvin, 2013).

153 Two previous studies have evaluated TRMM products for the Tien Shan Mountains.

154 One compared TRMM with every rain gauge in Kyrgyzstan (Karaseva et al., 2012);

155 the other examined basins in the mid Tien Shan Mountain range (Ji and Chen, 2012).

156 Both found that TRMM underestimated precipitation in mountainous areas and

157 during heavy precipitation events, possibly due to difficulties in detecting shallow,

158 orographic rainfall (Adler et al., 2003). Aspect was found to be an important factor

159 with south facing slopes having higher accuracy and correlation compared with north

160 facing slopes. However, there is low confidence in this finding because of limited

161 data for south facing slopes (Ji and Chen, 2012). Karaseva et al. (2012) report low

162 correlations in the vicinity of large lakes (e.g., Issyk Kul and Toktogul) due to

163 contamination of the microwave signal by water bodies and mountains within the

164 sensor footprint. Strongest correlations were found in the high plateaus, including for

165 the Naryn gauge (Karaseva et al., 2012).

166 Rain gauge data are incorporated differently depending on aggregation period. The

167 3B43 (V7) (monthly precipitation estimate) is produced by first summing original

168 three-hour values by calendar month. Second, monthly precipitation gauge analysis

169 is used to create a large scale bias adjustment to the satellite estimates. Lastly,

170 monthly gauge adjusted satellite estimates are combined directly with gauge

171 precipitation via inverse error variance weighting to create the final product. The

172 3B42 (V7) dataset (daily precipitation estimate) is derived by scaling the original

173   three-hourly estimates so they sum approximately to the monthly gauge adjusted

174   satellite-gauge combination value calculated in step two of the 3B43 (V7) procedure

175   (Huffman and Bolvin, 2013). Henceforth, we refer to 3B42 (V7) as daily TRMM, and

176   3B43 (V7) as monthly TRMM.

177   Monthly and daily TRMM were obtained at 0.5° resolution from the TRMM Online

178   Visualisation and Analysis System (TOVAS) for every cell in the Naryn basin for the

179   years 1998 to 2010 inclusive. In addition, monthly and daily data were downloaded

180   for the same time period but at 0.25° resolution for cells within the 0.5° grid nearest

181   to the Naryn meteorological station (**Figure 1**).

182

183   **2.2 Ground-based measurements**

184   Daily meteorological and hydrological data were collected as part of a European

185   Bank for Reconstruction and Development (EBRD) project investigating downstream

186   consequences of climate change and flow regulation on the River Naryn (Wilby et al.,

187   2011). Daily precipitation totals and mean daily temperature were obtained for the

188   meteorological station at Naryn for the years 1981 to 2010 (**Figure 1**). This single

189   station was chosen for two reasons. First, an earlier analysis of all stations in

190   Kyrgyzstan showed that the correlation between TRMM and gauge precipitation was

191   strongest at Naryn (Karaseva et al., 2012). Second, the site is centrally located

192   within the Naryn basin, and the record is unbroken for the period over-lapping with

193   river flow data. Daily discharges were obtained for a site upstream of Toktogul for the

194   years 2000 to 2009. The inflow record has several months with missing data which

195   were filled by interpolating from monthly mean values.

196

197   **3 Methods**

198   The analysis proceeded in two stages. First, we evaluated the quality of daily and

199   monthly remotely sensed (TRMM) precipitation estimates in the vicinity of the Naryn

200   meteorological station. Second, we assessed the feasibility of forecasting monthly

201   inflows to Toktogul based on a blend of remotely sensed and ground-based

202   observations. Each step is described below.

7

3.1 Evaluation of TRMM products

204 We extend earlier analyses by comparing Naryn and TRMM precipitation at different

205 spatial and temporal resolutions. We recognise that it is not possible to undertake a

206 fully independent test of TRMM in data sparse regions because it is likely that data

207 from available meteorological stations have been assimilated by the algorithm.

208 Inspection of the gauges used for Kyrgyzstan confirms that this is the case[2].

209 Consistent with other networks in the post-Soviet era, the number of gauges

210 assimilated by TRMM declined from 23 (1998) to 12 (2010), but data for the station

211 at Naryn was blended with other sites throughout our study period (**Figure 2**).

212 With these points in mind we investigated specific instances in which there are major

213 discrepancies between TRMM and Naryn gauge data. Monthly mean and annual

214 precipitation totals were calculated for the 0.5° TRMM cell overlying the Naryn

215 meteorological station for the years 1998 to 2010. Likewise, cumulative precipitation

216 totals and distributions were derived for the nearest 0.25° and 0.5° TRMM cells for

217 the same period. The false alarm ratio was calculated for each month as the fraction

218 of days on which TRMM detects precipitation but the gauge did not, divided by the

219 total number of days on which TRMM measured precipitation (Scheel et al., 2011).

220 Next, the non-parametric Spearman rank correlation coefficient was estimated using

221 daily time series for the same cells. This was followed by a wider analysis of

222 covariance across all cells in the Naryn basin in which data were stratified by

223 calendar month and season. Finally, all cells, permutations of concurrent and lagged

224 (0 to 3 months) TRMM precipitation, and moving averages (0 to 6 months) were

225 correlated with monthly river flow at Toktogul. This was undertaken in order to

226 identify the TRMM cell(s) and area(s) of the basin, lag interval (t), and averaging

227 period (m) that potentially yield predictability of inflows.

228

3.2 River flow estimation

230 Following earlier studies we evaluated various combinations of predictor variable,

231 averaging period and lag interval to develop multiple-linear regression models of

---

[2] The GPCC visualizer enables inspection of sites used in TRMM:
http://kunden.dwd.de/GPCC/Visualizer

232 monthly inflow to Toktogul for the period May 1999 to July 2010 (Schär et al., 2004;

233 Archer and Fowler, 2008; Magar and Jothiprakash, 2011; and Pal et al., 2013).

234 Available monthly variables were precipitation and temperature observations at

235 Naryn, basin average TRMM precipitation, lagged and time-averaged TRMM

236 precipitation from individual cells, and dummy variable for month to capture the

237 annual cycle (**Table 1**). The dummy variable regression weights give the flow

238 anomaly with respect to a reference month (in this case December) once the

239 influence of other predictors has been accounted for.

240 Regression modelling proceeded in two steps. First, the large number of lagged,

241 time-averaged and spatially-explicit candidate variables was reduced to a smaller set

242 of statistically significant, independent predictors. Second, the forecast skill of

243 chosen predictors was determined using cross-validation. These stages ensure that

244 the most parsimonious models, with out of sample forecast skill, are constructed.

245 We began by examining simple linear regression relationships between runoff in the

246 summer snow melt season (April to September) as a function of individual predictors:

247 year, precipitation, temperature and runoff in the preceding winter (October to

248 March). This split-year approach has been applied to other runoff records in Central

249 Asia and informs the preliminary selection of candidate predictor variables for sub-

250 seasonal forecast models (e.g., Schär et al., 2004; Pal et al., 2013). Preferred

251 *monthly* variables were then screened by stepwise multiple-linear regression,

252 terminating at the point where inclusion of additional variables did not improve the

253 amount of explained variance (when adjusted for sample size and number of

254 predictors). Optimal sets of predictors of monthly discharge (Q) were identified for

255 concurrent (t), one (t+1), two (t+2) and three (t+3) months lead time.

256 Regression model skill was then assessed using cross-validation by which monthly

257 *Q* for individual years was predicted using models built on other years of data. For

258 instance, flows for the year April 1999 to March 2000 would be predicted by a model

259 calibrated on data for April 2000 to March 2010. Year-by-year a full series of

260 predicted flows was built enabling validation against data not used in model

261 calibration. Available records for Toktogul and TRMM permit cross-validation of 11

262 year-long segments of data, each with their own regression parameter sets. This

263 provides a more stringent test of model skill than measures of calibration fit to the

9

264   whole data. Note that, however, an operational version of the model would be fit to

265   the selected predictor set using the entire record then recalibrated periodically as

266   more data become available.

267   All model predictions were benchmarked with respect to the Zero Order Forecast

268   (ZOF): the amount of explained variance that can be obtained from the simplest

269   possible model – in this case the long-term monthly mean flow. For comparability,

270   identical segments of data were used for estimating the long-term mean as those

271   entered into the 11 cross-validated regression models. The *HydroTest* tool (Dawson

272   et al., 2007) was used to derive five metrics of model forecast skill: Root Mean

273   Squared Error (RMSE); A Information Criteria (AIC); Nash-Sutcliffe Coefficient (NSC);

274   Percentage Error in Peak (PEP); and the Mean Absolute Relative Error (MARE).

275

4 Results

277   With the caveat about lack of full independency of data in mind, we first assessed

278   realism of TRMM precipitation estimates at different temporal scales using the gauge

279   data at Naryn. These data were then used to build and validate models of monthly

280   inflows to Toktogul with forecast horizons of up to three months.

281

4.1 Evaluation of TRMM products

283   When compared with gauge precipitation at Naryn, 0.5° TRMM estimates totals

284   during the accumulation (October to March) and melt-season (April to September)

285   with -1% and +11% bias respectively. The equivalent biases for the nearest 0.25°

286   TRMM cell are -2% and +5%. The largest over-estimation by TRMM occurs in July,

287   August and September (**Figure 3a**). Conversely, 0.5° TRMM April totals

288   underestimate gauge totals by 16%. The monthly false alarm ratio for daily

289   precipitation occurrence varied between 0.41 (March) and 0.67 (September).

290   **Figure 3b** shows the variability in annual gauge precipitation with 2003 having more

291   than twice the total of 2006. TRMM overestimates the annual total in the majority of

292   years, however, monthly time-series show strong correlation with the gauge at both

293   0.25° TRMM (r=0.86) and 0.5° TRMM (r=0.86) resolutions (**Figure 4**). Overall, the

10

294 correlation between monthly gauge and TRMM is strongest in February, September

295 and November (r=0.94) and weakest in May (r=0.16) and July (r=0.66). This is

296 explained by three significant discrepancies which occurred in May 2003, July 2006

297 and July 2010 when 0.5° TRMM overestimates gauge totals by 72.1%, 99.7% and

298 199.6% respectively. Over the course of the 13 year period, 0.25° TRMM and 0.5°

299 TRMM over-estimate the cumulative total at Naryn by 5% and 10% respectively with

300 the departure beginning at the May 2003 anomaly (**Figures 5**).

301 Consistent with earlier studies (Karaseva et al., 2012; Ji and Chen, 2012), TRMM

302 over-estimates the frequency of light precipitation days, and under-estimates the

303 occurrence of heavy precipitation (**Figure 6**). However, it is evident that 0.25° TRMM

304 provides a better match to the cumulative percentile distribution than 0.5° TRMM.

305 The correlation between daily gauge and TRMM totals is weak (r=0.25) compared

306 with monthly totals (r=0.93) (**Figure 7**). This is to be expected because the bias

307 correction procedure within TRMM scales sub-daily amounts such that their monthly

308 aggregate converges with that of the monthly gauge total (Huffman et al., 2007).

309 The strength of correlation between gauge precipitation and 0.5° TRMM totals varies

310 with distance from the meteorological station. Marginally stronger correlations are

311 found in upwind TRMM cells for daily series (**Figure 8a**), and to the north and west

312 of Naryn for monthly series (**Figure 8b**). These correlation surfaces show the extent

313 to which the record at Naryn might be representative of precipitation elsewhere in the

314 basin (assuming that TRMM values are 'truth').

315

316 **4.2 River flow estimation**

317 Discharge in the summer half-year (April to September) is significantly related to

318 winter TRMM precipitation totals averaged across the Naryn basin (PA) or over the

319 most sensitive sub-basin (PO) (**Table 2**). Precipitation measured at Naryn and

320 antecedent discharge are weakly related to summer flow (but are statistically

321 insignificant predictors since $p > 0.05$). Winter temperatures at Naryn and time (year)

322 have no predictive skill over the fit period. This is consistent with the findings of

323 Schär et al. (2004) and Schiemann et al. (2007) for the Syr Darya as a whole.

324 Monthly discharge typically rises from a minimum in February to maximum in June.

325 However, peak flows are subdued during low precipitation years such as 2007 and

326 2008, arrive earlier in warm years (2006), or later in cold years (2009) (**Figure 9**).

327 This inter-annual variability would not be captured by a ZOF based on the long-term

328 monthly mean flow alone. Nonetheless, the ZOF still explained 81% of the variance

329 in monthly discharge entering Toktogul and sets a challenging minimum standard for

330 evaluating more elaborate models.

331 **Figure 10** shows the amount of variance in monthly discharge explained by TRMM

332 for different lag intervals (zero to three months). The cells with greatest explained

333 variance at zero lag include eastern mountain areas with seasonal snow cover and

334 glacier storage, as well as Song-Kul Lake (cell 41.5°N, 74.75°E) during the melt

335 season. As the length of lag interval increases the zone producing greatest

336 predictability migrates westwards. Even at forecast horizon t+3 the amount of

337 variance in flows explained by TRMM still exceeds 30%.

338 The correlation between river flow and candidate predictors was assessed by

339 systematically varying lead-time (t+0 to t+3 months) and averaging period (1 to 6

340 months) for monthly temperature and precipitation at Naryn, the TRMM basin

341 average precipitation, and the optimum TRMM cell(s) (identified from **Figure 10**).

342 The correlation coefficient for temperature is strongest with no lead-time (t+0) or

343 smoothing (r=0.73) (**Figure 11**). Greater lead-times and longer averaging periods

344 show weak but statistically significant correlations (r>0.17) that eventually become

345 negative as the temperature and flow regimes are in anti-phase.

346 The correlation with Naryn precipitation is strongest for t+0 when averaged over the

347 previous three months (r=0.74) (**Figure 11**). Lead-time t+1 correlations are

348 strengthened by averaging over two months (r=0.68). The correlation is statistically

349 significant up to t+3 months if there is no averaging (r=0.28). Lead-time correlations

350 are strengthened (relative to Naryn) when applying basin area or optimum TRMM

351 cells. For comparison, these predictors yield significant t+3 (no-averaging)

352 correlations r=0.39 and r=0.43 respectively. Regardless of the averaging period, no

353 significant correlations were found for any TRMM product (whether single cell or

354 basin average) beyond t+3, indicating a limit to predictability from this data source.

355 Estimation of current flows (Q0) was improved by including antecedent discharge

356 and TRMM precipitation from the most highly correlated cell (smoothed over four

357 months) alongside the monthly dummy variable (**Tables 3** and **4**). The best predictor

358 set for the one month ahead flow forecast model (Q1) also includes temperature

359 (lag-1) (**Tables 3** and **4**). Regression fit remains superior to the ZOF fit for two (Q2)

360 and three (Q3) month lead-times but these do not incorporate antecedent

361 temperatures. In fact, temperature explains only 9% and 1% of the variation in flow

362 at t+2 and t+3 months respectively. Only the optimum TRMM cell provides

363 predictability in Q3 beyond that which can be achieved by the monthly mean flow

364 alone (**Tables 3** and **4**).

365 Given the limited data, cross-validation was used to compare predictive skill of

366 regression models relative to the ZOF over forecast horizons t+1 to t+3 months

367 (**Figure 12**). According to the chosen performance metrics, Q1, Q2 and Q3 models

368 are superior to ZOF for all diagnostics, except the MARE for Q3 (**Table 5**). Hence,

369 regression models have lower RMSE and AIC and higher NSC than the ZOF up to

370 Q3. Regression models also have lower errors in the estimated peak, even though

371 these are still under-predicting by typically 20 to 30% (compared with 35% for ZOF).

372 The circumstances under which there are large (t+1) forecast errors were explored

373 through closer inspection of daily series of precipitation at Naryn and daily inflow at

374 Toktogul (**Figure 13**). For example, the forecasted peak monthly flow in 2002 is too

375 low and too late (see Q1 model in **Figure 12**) because heavy precipitation in late

376 June 2002 is smoothed and lagged by the model such that it impacts estimated flows

377 in July 2002. In this case, the monthly time-step of the model is simply too coarse to

378 resolve the observed near synchronous daily rainfall-runoff response in June. Other

379 discrepancies may be attributed to interpolation of missing daily flows from monthly

380 means (such as the overestimation of discharge during June to September 2007).

381

5 Discussion

383 Here we interpret our results in the context of other river flow forecast models

384 developed for the region, and from physical reasoning about the underlying hydro-

385 climatic processes.

13

386

5.1 Evaluation of TRMM products

388 The quality of TRMM products has been reviewed elsewhere from the perspective of
389 skill linked to temporal and spatial resolution (Scheel et al., 2011) or physical
390 environment (Berg et al., 2006); performance and corrections needed in
391 mountainous terrain (Condom et al., 2011; Matzler and Standley, 2000; Ji and Chen,
392 2012); local micro-meteorological and orographic effects (Petty, 2001; Barros et al.,
393 2004); snowfall detection and evaluation (Gebremichael et al., 2010; Ji and Yu,
394 2013); and utility for hydrologic prediction (Yong et al., 2012).

395 These studies show that assessing the quality of remotely sensed precipitation
396 estimates is not straightforward. First, lack of ground measurements limits scope to
397 'ground truth' satellite data (Ebert et al., 2007). Some studies resort to spatial
398 interpolation to infill between stations, but this introduces additional uncertainties (Ji
399 and Chen, 2012). Second, interpretations are complicated when comparing point
400 measurements from gauges with area-averages from satellites because spatial
401 averaging can lead to over-estimation of precipitation occurrence or reduce the
402 magnitude of extreme events relative to local observations (Scheel et al., 2011).
403 Third, gauge data are accumulated over fixed intervals (such as 3-hourly or daily
404 totals) whereas TRMM is a snapshot measurement (Scheel et al., 2011).

405 Good agreement between the Naryn gauge and TRMM precipitation during the
406 accumulation period implies that the latter is able to estimate snowfall totals well at
407 this site (**Figure 3**). This is contrary to some studies that assert TRMM should not be
408 used without calibration for snowfall (Gebremichael et al., 2010; Yong et al., 2012). It
409 is possible that the rate applied to snowfall (0.1 mm hour^{-1}) is close to that observed
410 at Naryn which, along with relatively low totals during winter months, results in a
411 small absolute bias. However, it must be kept in mind that the accuracy of the gauge
412 for snowfall is also unknown. Therefore, it is unclear whether the gauge or TRMM
413 estimate for May 2003 is most trustworthy. TRMM gave 40 mm of precipitation on
414 one day whilst the gauge recorded zero, followed by two days of rainfall measured
415 by the gauge totalling 30 mm that TRMM estimated to be less than 5 mm. It is
416 conceivable that during this time very few if any of the TMPA instruments covered
417 the study area, thereby reducing the accuracy of the TRMM estimate (Huffman et al.,

418 2007). Alternatively, observed precipitation may have been aggregated over more

419 than one day or entered incorrectly against these dates.

420 TRMM overestimated the frequency of occurrence (not shown) and total precipitation

421 in July, August and September (**Figure 3**). The relatively high false alarm ratio at this

422 time could be linked to localised heavy precipitation events under southerly monsoon

423 airflows. Such events may be detected by the area estimates of TRMM but were

424 missed by point measurements at the gauge (Bothe et al., 2012; Bell and Kundu,

425 2003; Bowman, 2004). This is supported by the fact that the highest overestimation

426 occurred in the lower half of the 0.5° TRMM cell – the area furthest from the gauge.

427 The correlation surfaces (**Figure 8**) partly reflect the time-varying influence of

428 neighbouring gauges within the domain. Overall, the r≥0.7 correlation field (i.e., more

429 than 50% variance explained) for monthly amounts covers 21 out of 35 cells in the

430 study area (**Figure 8b**). In other words, the Naryn record is strongly correlated with

431 TRMM precipitation estimates over approximately 60% of the basin area. The Naryn

432 record is least representative of TRMM values in the Fergana Range (the southwest

433 portion of the basin, **Figure 1**). Karaseva et al. (2012) and the GPCC visualizer show

434 a cluster of five gauges in this area (**Figure 2**) which presumably exert a stronger

435 influence than Naryn on local TRMM estimates.

436

5.2 River flow estimation

438 A growing number of studies are exploring the application of remotely sensed

439 information in hydrological modelling (e.g., Yilmaz et al., 2005; Artan et al., 2007; Su

440 et al., 2008; Bookhagen and Burbank, 2010; Stisen and Sandholt, 2010; Wilby and

441 Yu, 2013). Previous research shows that model skill can be improved by bias

442 correcting TRMM precipitation estimates, or by blending TRMM with gauge data to

443 simulate runoff (Yu et al., 2011; Bitew et al., 2012). Many studies have focused on

444 large scale modelling (medium/ large basins to global scale); relatively few examine

445 the utility of satellite data for runoff simulation at smaller scales (Hong et al., 2007a;

446 Milewski et al., 2009). It is also recognised that different satellite products can yield

447 different river flow simulations even when passed through the same hydrological

448 model (Chintalapudi et al., 2012). Arid and semi-arid basins can be particularly

449 challenging to model with satellite precipitation estimates because of localised,

450 heavy precipitation events, coupled with strongly non-linear rainfall-runoff processes

451 (Sagintayev et al., 2012).

452 Earlier research into river flows within the Naryn/Syr Darya basins examined how

453 climate change could impact water resources with and without adaptation (e.g.,

454 Siegfried et al., 2012; Ismaiylov et al., 2007; Wilby et al., 2011). Others have used

455 satellite precipitation estimates to calibrate models. For example, Immerzeel et al.

456 (2012) applied a conceptual model with PERSIANN satellite precipitation inputs to

457 assess climate change impacts on water resources. Pereira-Cardenal et al. (2011)

458 used TRMM precipitation with radar altimetry to produce near real-time simulations

459 of Toktogul reservoir water levels.

460 Savoskul et al. (2003) observed that a substantial fraction of winter precipitation

461 contributes to runoff with delay due to seasonal and perennial storage of

462 precipitation in snow and ice. Onset of snowmelt occurs later in the year at higher

463 elevations so these regions might be expected to contribute at longer lag intervals.

464 This is indeed the case, with strongest correlations for delayed runoff from the

465 mountain ranges in the north and southwest of the basin. A further factor is the

466 spatial variation in magnitude of the spring peak in precipitation. Aizen et al. (1996;

467 1997) report that areas below 2,500 m have two maxima with the main occurring

468 between March-May; whereas areas above 2,500 m have a single maximum

469 between May-July. They also noted that the proportion of annual precipitation

470 occurring during spring varies from 35-45 % in areas below 2,500 m compared to 45-

471 55 % above 2,500 m.

472 Schär et al. (2004) assumed that accumulated runoff for the Syr Darya in summer

473 (May to September) is a linear function of accumulated precipitation in the preceding

474 winter and spring (December to February, March and April). Temperature potentially

475 influences contributions from glacier melt, timing of melt season onset and proportion

476 of total precipitation in liquid state. However, their stepwise regression model of

477 summer runoff omitted all temperature variables, depending instead on precipitation

478 during winter (December to February), March and April alone despite a high degree

479 of glaciation of the test basin.

480 Predictability of summer flows into Toktogul appears to be maximised by using

481 TRMM precipitation estimates for the cell over Song-Kul Lake (**Figure 1**). The TRMM

482 basin average for winter also surpassed observed precipitation at Naryn as a

483 predictor. This suggests that seasonal inflows to Toktogul may be routinely

484 forecasted using publicly available satellite products and regression models akin to

485 those shown in **Table 2**. As more satellite and river flow data become available it will

486 be possible to re-evaluate the stationarity of model parameters, and to discern

487 possible long-term augmentation of summer flow by glacier wastage (Kriegel et al.,

488 2013).

489 In the meantime, temperature was found to be a statistically insignificant predictor of

490 summer discharge and was retained in only one of the four monthly models

491 developed for the Naryn (**Tables 3** and **4**). Once the seasonal snow and ice melt

492 regime is captured by the monthly dummy variable, the remaining temperature effect

493 is negative: months preceded by higher air temperatures typically have lower than

494 average runoff. This could be interpreted as earlier onset of melting, greater

495 evaporative losses at lower elevations, or as reflecting the weak negative correlation

496 (r=-0.27) between summer temperature and precipitation. A negative (but statistically

497 non-significant) regression parameter between air temperature and summer runoff

498 has also been reported for the Syr Darya to Chinaz (Schiemann et al., 2007). More

499 generally, positive temperature anomalies and suppressed summer convective

500 precipitation over Central Asia are associated with strong Indian summer monsoons

501 (Schiemann et al., 2007).

502

503 **6 Conclusions**

504 The purpose of this paper was to explore the feasibility of forecasting monthly and

505 seasonal reservoir inflows given minimal surface data and remotely sensed (TRMM)

506 precipitation estimates. Toktogul reservoir was chosen to test the approach because

507 of the economic significance of the structure, and importance to the region's highly

508 complex water management system (Karaev, 2005; Kraak, 2012b). Previous studies

509 have evaluated aspects of TRMM for Kyrgyzstan and the wider region; others have

510 investigated the potential for seasonal forecasting of runoff for large basins in Central

511   Asia. We refined these analyses by showing how predictive skill might be maximised

512   through judicious selection of TRMM cell(s), averaging and lag intervals.

513   Despite the simplicity of the models and limited data requirements over 80% of the

514   variance in monthly inflows is explained with three month lead, and up to 65% for

515   summer half-year flows based on TRMM estimates of winter precipitation. In line with

516   earlier research, temperature was found to have limited predictive skill at monthly

517   scales, and no skill for seasonal forecasting Naryn flows. The sub-basin feeding the

518   major tributary below Song Kol Lake was shown to have significant influence on

519   inflows during the melt season and is a priority location for long-term monitoring.

520   Indeed, any remaining meteorological stations in the vicinity (41° 50'N, 75° 10'E)

521   should be protected from closure, and the area prioritised for network expansion.

522   Despite the parsimony of the regression models there may be good reasons for

523   parallel development of non-linear statistical or deterministic algorithms (such as the

524   Snowmelt Runoff Model (SRM) which has already been implemented for the Naryn

525   basin) (Wilby et al., 2011). These models could assimilate remotely sensed snow

526   cover for initialising forecasts of runoff over days to weeks ahead, driven by

527   numerical weather predictions of precipitation and temperature. In this way,

528   probabilistic forecasts of extreme inflows could be issued by deploying ensemble

529   predictions of inputs and SRM parameter sets. Snow and ice budgeting can also be

530   used to carry-over mass balance changes between successive melt seasons and to

531   investigate the observed long-term deglacierization of the Naryn due to prolongation

532   of the melt season (Kriegel et al., 2013).

533   We demonstrated the possibility of forecasting reservoir inflows using TRMM

534   precipitation estimates but the approach remains the same regardless of the satellite

535   products employed. Key steps include evaluating precipitation estimates against

536   available surface data at various time and space scales, then selecting those parts of

537   the river basin that yield greatest predictability for specified forecast horizons.

538   Credibility of the statistical model(s) is strengthened where physically sensible

539   explanations can be given for the prediction skill, and when stationarity of model

540   parameters has been tested through cross-validation techniques. Although the

541   TRMM satellite is expected to cease operating in February 2016 the successor

542   and/or other precipitation estimates could be calibrated then used in operational flow

543   forecasts for strategically important water infrastructure in Central Asia.

544   Finally, beyond river flow, other environmental hazards affecting reservoir operations

545   may be predictable from satellite products. For instance, peak occurrence for

546   landslides and mudflows tends to be associated with rising temperatures and heavy

547   rainfall in spring. This opens the potential for predicting rainfall-triggered landslides

548   (including mud and debris flows) from real-time satellite imagery (as in Hong et al.,

549   2006; 2007b; 2007c). The Goddard Space Flight Center already provides global

550   maps of potential landslide areas based on rainfall estimates with 1, 3 and 7 day

551   lead time[3]. Potential contingency measures that could be taken at individual

552   hydropower plants include draw down of reservoir level to increase freeboard for

553   flood waves induced by channel blockage or debris slides.

554

Acknowledgements

---

[3] http://trmm.gsfc.nasa.gov/publications_dir/potential_landslide.html

References

561   **References**

562   Adler, R.F. Huffman, G.J., Chang, A., Ferraro, R., Xie, P.P., Janowiak, J., Rudolf, B.,
563   Schneider, U., Curtis, S., Bolvin, D., Gruber, A., Susskind, J., Arkin, P. and Nelkin, E.
564   (2003). The Version-2 Global Precipitation Climatology Project (GPCP) Monthly
565   Precipitation Analysis (1979–Present). *Journal of Hydrometeorology*, 4 (6), 1147–
566   1167.

567   Aizen, E.M., Aizen, V.B., Melack, J.M., Nakamura, T. and Ohta, T. (2001).
568   Precipitation and atmospheric circulation patterns at mid-latitudes of Asia.
569   *International Journal of Climatology*, 21, 535-556.

570   Aizen, V.B., Aizen, E.M and Melack, J.M. (1995a). Climate, snow cover, glaciers and
571   runoff in the Tien Shan, Central Asia. *Water Resources Bulletin*, 31 (6), 1113-1129.

572   Aizen, V.B., Aizen, E.M. and Melack, J.M. (1995b). Characteristics of runoff
573   formation at the Kirgizskiy Alatoo. *Proceedings of a boulder Symposium (IAHS*
574   *Publications)*. 228, 413-430.

575   Aizen, V.B., Aizen, E.M and Melack, J.M. (1996). Precipitation, melt and runoff in the
576   northern Tien Shan. *Journal of Hydrology*, 186, 229-251.

577   Aizen, V.B., Aizen, E.M., Melack, J.M. and Dozier, J. (1997). Climate change
578   impacts on glaciers and runoff in Tien Shan (Central Asia).*Journal of Climate*, 10 (6),
579   1393-1404.

580   Archer, D.R. and Fowler, H.J. 2008. Using meteorological data to forecast seasonal
581   runoff on the River Jhelum, Pakistan. *Journal of Hydrology*, **361**, 10-23.

582   Artan, G. Gadain, H., Smith, J.L., Asante, K., Bandaragoda, C.J. and Verdin, J.P.
583   (2007). Adequacy of satellite derived rainfall data for stream flow modeling. *Natural*
584   *Hazards*, 43, 167-185.

585   Balthrop, C. and Hossain, F. (2010). Short note: A review of state of the art on
586   treaties in relation to management of transboundary flooding in international river
587   basins and the Global Precipitation Measurement mission. *Water Policy*, 12, 635-
588   640.

589   Barros, A.P., Kim, G., Williams, E. and Nesbitt, S.W. (2004). Probing orographic

590   controls in the Himalayas during the monsoon using satellite imagery. *Natural*

591   *Hazards and Earth System Sciences*, 4, 29–51.

592   Bell, T.L. and Kundu, P.K. (2003). Comparing satellite rainfall estimates with rain

593   gauge data: Optimal strategies suggested by a spectral model. *Journal of*

594   *Geophysical Research: Atmospheres*, 108, 4121.

595   Berg, W., L'Ecuyer, T. and Kummerow, C. (2006). Rainfall Climate Regimes: The

596   Relationship of Regional TRMM Rainfall Biases to the Environment. *Journal of*

597   *Applied Meteorology and Climatology*, 45, 434-454.

598   Bitew, M.M., Gebremichael, M., Ghebremichael, L.T. and Bayissa, Y.A. (2012).

599   Evaluation of High-Resolution Satellite Rainfall Products through Streamflow

600   Simulation in a Hydrological Modeling of a Small Mountainous Watershed in

601   Ethiopia. *Journal of Hydrometeorology*, 13, 338–350.

602   Bookhagen, B. and Burbank, D.W. (2010). Toward a complete Himalayan

603   hydrological budget: Spatiotemporal distribution of snowmelt and rainfall and their

604   impact on river discharge. *Journal of Geophysical Research*, 116, 1-25.

605   Bothe, O., Fraedrich, K. and Zhu, X. (2012). Precipitation climate of Central Asia and

606   the large-scale atmospheric circulation. *Theoretical and Applied Climatology*, 108 (3-

607   4), 345-354.

608   Bowman, K.P. (2004). Comparison of TRMM precipitation retrievals with rain gauge

609   data from ocean buoys. *Journal of Climate*, 18, 178-190.

610   Chintalapudi, S., Sharif, H.O., Yeggina, S. and Elhassan, A. (2012). Physically

611   based, hydrologic model results based on three precipitation products. *Journal of the*

612   *American Water Resources Association*, 48 (6), 1191–1203.

613   Collischonn, B. and Pante, A.R. (2011). TRMM-forced rainfall—runoff modelling for

614   water management purposes in small ungauged basins. *IAHS-AISH publication*.

615   ISSN- 0144-7815.

616 Condom, T., Rau, P. and Espinoza, J.C. (2011). Correction of TRMM 3B43 monthly
617 precipitation data over the mountainous areas of Peru during the period 1998–
618 2007. *Hydrological Processes*, 25, 1924–1933.

619 Dawson, C.W., Abrahart, R.J. and See, L.M. 2007. HydroTest: A web-based toolbox
620 of evaluation metrics for the standardised assessment of hydrological forecasts.
621 *Environmental Modelling and Software*, 22, 1034-1052.

622 Ebert, E.E., Janowiak, J.E. and Kidd, C. (2007). Comparison of Near-Real-Time
623 Precipitation Estimates from Satellite Observations and Numerical Models. *American
624 Meteorological Society*, 88, 47-64.

625 Gebremichael, M., Anagnostou, E.N. and Bitew, M.M. (2010). Critical Steps for
626 Continuing Advancement of Satellite Rainfall Applications for Surface Hydrology in
627 the Nile River Basin. *Journal of the American Water Resources Association*, 46, 361-
628 366.

629 Hirpa, F.A., Hopson, T.M., De Groeve, T., Brakenridge, G.R., Gebremichael, M. and
630 Respreto, P.J. (2013). Upstream satellite remote sensing for river discharge
631 forecasting: Application to major rivers in South Asia. *Remote Sensing of
632 Environment*, 131, 140-151.

633 Hodgson, S. (2010). *Strategic Water Resources in Central Asia: in search of a new
634 international legal order.* Centre for European Policy Studies, Policy Brief No.14.
635 Madrid, Spain, 6pp.

636 Hong, Y., Adler, R. and Huffman, G. (2006). Evaluation of the potential of NASA
637 multi-satellite precipitation analysis in global landslide hazard assessment.
638 *Geophysical Research Letters*, 33, L22402.

639 Hong, Y., Adler, R.F., Hossain, F. Curtis, S. and Huffman, G.J. (2007a). A first
640 approach to global runoff simulation using satellite rainfall estimation. *Water
641 Resources Research*, 43, 1-8.

642 Hong, Y., Adler, R.F, Negri, A. and Huffman, G.J. (2007a). Flood and landslide
643 applications of near real-time satellite rainfall estimation. *Natural Hazards*, 43, 285-
644 294.

645   Hong, Y., Adler, R.F. and Huffman, G.J. (2007b). An experimental global monitoring
646   system for rainfall-triggered landslides using satellite remote sensing information.
647   *IEEE Trans. on Geosciences and Remote Sensing,* 45, 1671-1680.

648   Hopson, T.M. and Webster, P.J. (2010). A 1–10-Day Ensemble Forecasting Scheme
649   for the Major River Basins of Bangladesh: Forecasting Severe Floods of 2003-07.
650   *Journal of Hydrometeorology*, 11, 618-641.

651   Hossain, F., Katiyar, N., Wolf, A. and Hong, Y. (2007). The emerging role of satellite
652   rainfall data in improving the hydro-political situation of flood monitoring in the under-
653   developed regions of the world. *Natural Hazards*, 43 (2), 199-210.

654   Huffman, G.J. and Bolvin, D.T. (2013). *TRMM and Other Data Precipitation Data Set*
655   *Documentation.* Mesoscale Atmospheric Process Laboratory, NASA Goddard Space
656   Flight Center and Science Systems and Applications, Inc.
657   ftp://precip.gsfc.nasa.gov/pub/trmmdocs/3B42_3B43_doc.pdf. [Accessed
658   31/07/2013].

659   Huffman, G.J. Adler, R.F., Bolvin, D.T., Gu, G., Nelkin, E.J., Bowman, K.P., Hong,
660   Y., Stocker, E.F. and Wolff, D.B. (2007). The TRMM Multisatellite Precipitation
661   Analysis (TMPA): Quasi-Global, Multiyear, Combined-Sensor Precipitation Estimates
662   at Fine Scales. *Journal of Hydrometeorology*, 8, 38-55.

663   Hughes, D.A. (2006). Comparison of satellite rainfall data with observations from
664   gauging station networks. *Journal of Hydrology*, 327, 399-410.

665   Immerzeel, W.W., Lutz, A.F. and Droogers, P. (2012). Climate Change Impacts on
666   the Upstream Water Resources of the Amu and Syr Darya River Basins.
667   Wageningen, The Netherlands.

668   Immerzeel, W.W., van Beek, L.P.H. and Bierkens, M.F.P. (2010). Climate Change
669   Will Affect the Asian Water Towers. *Science*, 328, 1382-1385.

670   Ismaiylov, G.K., Federov, V.M. and Sadati Nezhad, S.D. (2007). Assessment of
671   possible anthropogenic changes in the runoff of the Syr Darya River on the basis of
672   a mathematical model. *Water Resources*, 34 (4), 359-371.

673 Ji, X. and Chen, Y. (2012). Characterizing spatial patterns of precipitation based on

674 corrected TRMM 3B43 data over the mid Tianshan Mountains of China. *Journal of*

675 *Mountain Science*, 9 (5), 628-645.

676 Ji, X. and Yu, Y. (2013). The influence of precipitation and temperature input

677 schemes on hydrological simulations of a snow and glacier melt dominated basin in

678 Northwest China. *Hydrology and Earth System Sciences Discussion Paper*, 10, 807-

679 853.

680 Karaev, Z. (2005). Water diplomacy in Central Asia. *Middle East Review of*

681 *International Affairs*, 9 (1), 63-69.

682 Karaseva, M.O., Prakash, S. and Gairola, R.M. (2012). Validation of high-resolution

683 TRMM-3B43 precipitation product using rain gauge measurements over

684 Kyrgyzstan. *Theoretical and Applied Climatology*, 108, 147-157.

685 Kekete, B.M., Vorosmarty, C.J., Roads, J.O. and Willmott, C.J. (2004). Uncertainties

686 in precipitation and their impact on runoff estimates. *Journal of Climate*, 17, 294-304.

687 Kraak, E. (2012a). *Central Asia's dam debacle.* Available:

688 http://www.chinadialogue.net/article/show/single/en/4790-Central-Asia-s-dam-

689 debacle. [Accessed 07/12/2013].

690 Kraak, E. (2012b). The Geopolitics of Hydropower in Central Asia: the Syr

691 Darya. *The Asia-Pacific Journal*, 105 (15).

692 Kriegel, D. Mayer, C., Hagg, W., Vorogushyn, S., Duethmann, D., Gafurov, A. and

693 Farinotti, D. (2013). Changes in glacierisation, climate and runoff in the second half

694 of the 20th century in the Naryn basin, Central Asia.*Global and Planetary Change*,

695 110, 51-61.

696 Magar, R.B. and Jothiprakash, V. (2011). Intermittent reservoir daily-inflow prediction

697 using lumped and distributed data multi-linear regression models. *Journal of Earth*

698 *Systems Science*, 120 (6), 1067-1084.

699 Matzler, C. and Standley, A. (2000). Relief effects for passive microwave remote

700 sensing. *International Journal of Remote Sensing*, 21, 2403–2412.

701   Milewski, A. Sultan, M., Yan, E., Becker, R., Abdeldayem, A., Soliman, F. and Gelil,

702   K.A. (2009). A remote sensing solution for estimating runoff and recharge in arid

703   environments. *Journal of Hydrology*, 373, 1-14.

704   NASA. (2011). *TRMM Senior Review Proposal.* Available:

705   http://pmm.nasa.gov/sites/default/files/document_files/TRMMSenRevProp_v1.2.pdf.

706   [Accessed 31/07/2013].

707   Pal, I., Lall, U., Robertson, A.W., Cane, M.A. and Bansal, R. (2013). Predictability of

708   Western Himalayan river flow: melt season inflow to Bhakra Reservoir in northern

709   India. *Hydrology and Earth System Sciences*, 17, 2131-2146.

710   Pereira-Cardenal, S.J., Riegels, N.D., Berry, P.A.M., Smith, R.D., Yakovlev, A.,

711   Siegfried, T.U. and Bauer-Gottwein, P. (2011). Real-time remote sensing driven river

712   basin modeling using radar altimetry. *Hydrology and Earth System Sciences*, 15,

713   241-254.

714   Petty, G.W. (2001). Physical and Microwave Radiative Properties of Precipitation

715   Clouds. Part II: A Parametric 1D Rain-Cloud Model for Use in Microwave Radiative

716   Transfer Simulations. *Journal of Applied Meteorology*, 40, 2115–2129.

717   Raskin, P., Hansen, E., Zhu, Z. and Stavisky, D. (1992). Simulation of Water Supply

718   and Demand in the Aral Sea Region. *Water International*, 17, 55-67.

719   Sagintayev, Z. Sultan, M., Khan, S.D., Khan, S.A., Mahmood, K., Yan, E., Milewski,

720   A. and Marsala, P. (2012). A remote sensing contribution to hydrologic modelling in

721   arid and inaccessible watersheds, Pishin Lora basin, Pakistan. *Hydrological*

722   *Processes*, 26 (1), 85–99.

723   Savoskul, O., Chevnina, E.V., Perziger, F.I., Vasilina, L.Y., Baburin, V.L., Danshin,

724   A.I., Matyakubov, B. and Murakaev, R.R. (2003). Water, climate, food, and

725   environment in the Syr Darya Basin, in Adaptation Strategies to Changing

726   Environments, Institute for Environmental Studies. Vrije University., Amsterdam.

727   Schär, C., Vasilina, L., Pertziger, F. and Dirren, S. (2004). Seasonal runoff

728   forecasting using precipitation from meteorological data assimilation systems.

729   *Journal of Hydrometeorology*, 5, 959-973.

730   Scheel, M.L.M. Rohrer, M., Huggel, C., Santos Villar, D., Silvestre, E. and Huffman,

731   G.J. (2011). Evaluation of TRMM Multi-satellite Precipitation Analysis (TMPA)

732   performance in the Central Andes region and its dependency on spatial and

733   temporal resolution. *Hydrology and Earth System Sciences*, 15, 2649-2663.

734   Schiemann, R., Glazirina, M.G. and Schär, C. (2007). On the relationship between

735   the Indian summer monsoon and river flow in the Aral Sea basin. *Geophysical*

736   *Research Letters*, 34, L05706.

737   Siegfried, T. Bernauer, T., Guiennet, R., Sellars, S., Robertson, A.W., Mankin, J.,

738   Bauer-Gottwein, P. and Yakovlev, A. (2012). Will climate change exacerbate water

739   stress in Central Asia? *Climate Change*, 112, 881–889.

740   Sorg, A., Bolch, T., Stoffel, M., Solomina, O., and Beniston, M. (2012). Climate

741   change impacts on glaciers and runoff in the Tien Shan (Central Asia). *Nature*

742   *Climate Change*, 2, 725–731.

743   Stisen, S. and Sandholt, I. (2010). Evaluation of remote-sensing-based rainfall

744   products through predictive capability in hydrological runoff modelling. *Hydrological*

745   *Processes*, 24 (7), 879–891.

746   Su, F., Hong, Y. and Lettermaier, D.P. (2008). Evaluation of TRMM Multisatellite

747   Precipitation Analysis (TMPA) and Its Utility in Hydrologic Prediction in the La Plata

748   Basin. *Journal of Hydrometeorology*, 9, 622-640.

749   Umaraliev, T. (2012). *Kyrgyzstan has energy crisis during very cold winter.* Available:

750   http://www.washingtontimes.com/news/2012/jan/27/kyrgyzstan-has-energy-crisis-

751   during-very-cold-wint/?page=all. [Accessed 20/07/2013].

752   UNDP. (2012). *Natural Disaster Risks in Central Asia.* Available:

753   http://europeandcis.undp.org/uploads/public1/files/vulnerability/Senior%20Economist

754   %20Web%20site/Policy%20brief_Natural%20Disaster%20Risks%20in%20Central%

755   20Asia.pdf. [Accessed 18/07/2013].

756   UNEP. (2008). The disappearance of the Aral Sea. In: Diop, S. and Rekacewicz,

757   P. *Vital Water Graphics - An Overview of the State of the World's Fresh and Marine*

758   *Waters.* 2nd ed. Nairobi, Kenya: UNEP.

759   Wilby, R.L. and Yu, D. (2013). Rainfall and temperature estimation for a data sparse

760   region. *Hydrology and Earth System Sciences*, 17, 3937-3955.

761   Wilby, R.L., Minikulov, N. and Rabb, B. (2011). *ANNEX 1: Modelling the climate-*

762   *sensitivity of rivers entering the Kairakkum and Nurek reservoirs, Tajikistan.*

763   Available: http://www.ppcr.tj/IP/Phase1/Component4/Annex%201.pdf. [Accessed

764   31/07/2013].

765   Yilmaz, K.K. et al. (2005). Intercomparison of Rain Gauge, Radar, and Satellite-

766   Based Precipitation Estimates with Emphasis on Hydrologic Forecasting. *Journal of*

767   *Hydrometeorology*, 6 (4), 497-517.

768   Yong, B. Hong, Y., Ren, L., Gourley, J., Huffman, G.J., Chen, X., Wang, W. and

769   Khan, S.I. (2012). Assessment of evolving TRMM-based multisatellite real-time

770   precipitation estimation methods and their impacts on hydrologic prediction in a high

771   latitude basin. *Journal of Geophysical Research*, 117, 1-21.

772   Yu, M., Chen, X., Li, L., Boa, A. and Jean de la Paix, M. (2011). Streamflow

773   Simulation by SWAT Using Different Precipitation Sources in Large Arid Basins with

774   Scarce Raingauges. *Water Resources Management*, 25, 2669–2681.

775   **Table 1** Variables used in regression models

$P_{t,n}$	Naryn meteorological station precipitation
$PA_{t,n}$	0.5° TRMM area average precipitation estimate
$PO_{t,n}$	0.5° TRMM optimum cell precipitation estimate
$T_{t,n}$	Naryn meteorological station temperature
$Q_{t,n}$	Discharge at Toktogul
t	Variable lag interval (*t* months)
n	Variable averaging period (*n* months)
M	Dummy variable for each calendar month (0 or 1)

776

777

778

779

780   **Table 2** Statistical estimates of the intercepts (α) and parameters (β) of simple linear

781   regression models, along with the amount of explained variance (R^2_{adj}), standard

782   error (SE) of the summer (April to September) runoff estimate (m^3s^{-1}) and model

783   significance level (*p*). All predictors except for time are for the winter half-year

784   (October to March).

Predictor	α (m^3s^{-1})	β	R^2_{adj} (%)	SE (m^3s^{-1})	*p* value
Time (year)	22993	-11.14	0	123	0.437
T	525	-28.83	0	123	0.418
P	473	12.67	22	107	0.096
PA	197	16.81	50	86	0.013
PO	247	17.85	65	71	0.003
Q	151	2.44	18	110	0.123

785

786   **Table 3** Summary of regression model predictor variables, explained variance (R^2_{adj})

787   and standard errors (SE) by forecast horizon (t+0 to t+3 months). In each case, the

788   final predictor set is shown in ***bold italics.*** See Table 1 for notations.

Model	Predictors	R^2_{adj} (%)	SE (m^3s^{-1})
ZOF	***M***	***81***	***147***
Q0 (t+0)	$PA_{0,4}$	42	258
	$T_{0,1}$	53	232
	$P_{0,3}$	54	228
	$Q_{1,1}$	59	217
	$PO_{0,4}$	73	174
	$Q_{1,1}, PO_{0,4}$	81	145
	$Q_{1,1}, PO_{0,4}, T_{0,1}$	84	137
	$M, Q_{1,1}, PO_{0,4}, T_{0,1}$	90	109
	$M, Q_{1,1}, PO_{0,4}$**	***90***	***109***
Q1 (t+1)	$T_{1,1}$	35	273
	$P_{1,1}$	37	268
	$P_{1,2}$	44	252
	$PA_{1,2}$	51	235
	$PO_{1,3}$	64	203
	$Q_{1,1}, PO_{1,3}$	70	185
	$Q_{1,1}, PO_{1,3}, T_{1,1}$	71	183
	$M, Q_{1,1}, PO_{1,3}$	89	111
	$M, Q_{1,1}, PO_{1,3}$**, ***$T_{1,1}$***	***89***	***110***
Q2 (t+2)	$T_{2,1}$	9	322
	$Q_{2,1}$	10	319
	$P_{2,1}$	30	283
	$PA_{2,1}$	43	254
	$PO_{2,1}$	48	242
	$Q_{2,1}, PO_{2,1}, T_{2,1}$	50	239
	$Q_{2,1}, PO_{2,1}$	49	240
	$M, Q_{2,1}, PO_{2,1}$**	***85***	***132***
Q3 (t+3)	$T_{3,1}$	1	336
	$Q_{3,1}$	1	336
	$P_{3,1}$	7	325
	$PA_{3,1}$	14	313
	$PO_{3,1}$	30	282
	$M, PO_{3,1}$***	***84***	***136***

789   Key: * cell 42°N 73.25°E; ** cell 41°N 73.25°E

790 **Table 4** Predictor variables and regression model parameters for monthly flow
791 forecast models Q0, Q1, Q2 and Q3 based on available data (May 1999 to July
792 2010). Model parameters shown in **bold** are statistically significant (p<0.05). Note
793 that the value of the dummy variable depends on prevailing month and may be
794 interpreted as the flow anomaly with respect to December (value zero).

Variable	Q0	Q1	Q2	Q3
Intercept	**-121.93**	-69.29	-39.78	**149.75**
Jan	-1.26	-114.16	22.63	**-134.57**
Feb	32.71	-119.44	53.88	**-129.37**
Mar	64.44	-20.24	109.82	-79.16
Apr	**147.01**	**214.50**	**272.65**	86.94
May	**348.53**	**546.26**	**580.59**	**460.67**
Jun	**455.48**	**659.18**	**771.21**	**728.37**
Jul	**185.64**	**399.02**	**477.50**	**530.45**
Aug	62.43	**263.15**	**218.87**	**284.05**
Sep	16.53	215.15	31.27	**147.83**
Oct	15.35	**198.81**	40.84	73.41
Nov	15.86	109.27	57.99	56.92
$Q_{1,1}$	**0.48**	**0.50**	-	-
$Q_{2,1}$	-	-	**0.35**	-
$PO_{0,4}$	**4.06**	-	-	-
$PO_{1,3}$	-	**2.54**	-	-
$PO_{2,1}$	-	-	**1.95**	-
$PO_{3,1}$	-	-	-	**2.31**
$T_{1,1}$	-	**-10.90**	-	-

795

796 **Table 5** Cross-validation results for ZOF, Q1, Q2 and Q3 models

Metric	ZOF	Q1	Q2	Q3
Root Mean Squared Error (RMSE) (m^3s^{-1})	151	118	139	144
A Information Criteria (AIC)	702	673	694	697
Nash-Sutcliffe Coefficient (NSC)	0.797	0.878	0.829	0.818
Percentage Error in Peak (PEP) (%)	-34.8	-21.4	-31.6	-27.7
Mean Absolute Relative Error (MARE) (%)	18.6	17.5	19.6	21.6

797

798

799

800 **Figure 1** a) Location of the River Naryn basin and Toktogul reservoir within
801 Kyrgyzstan; b) an elevation map of Kyrgyzstan.

802 a)
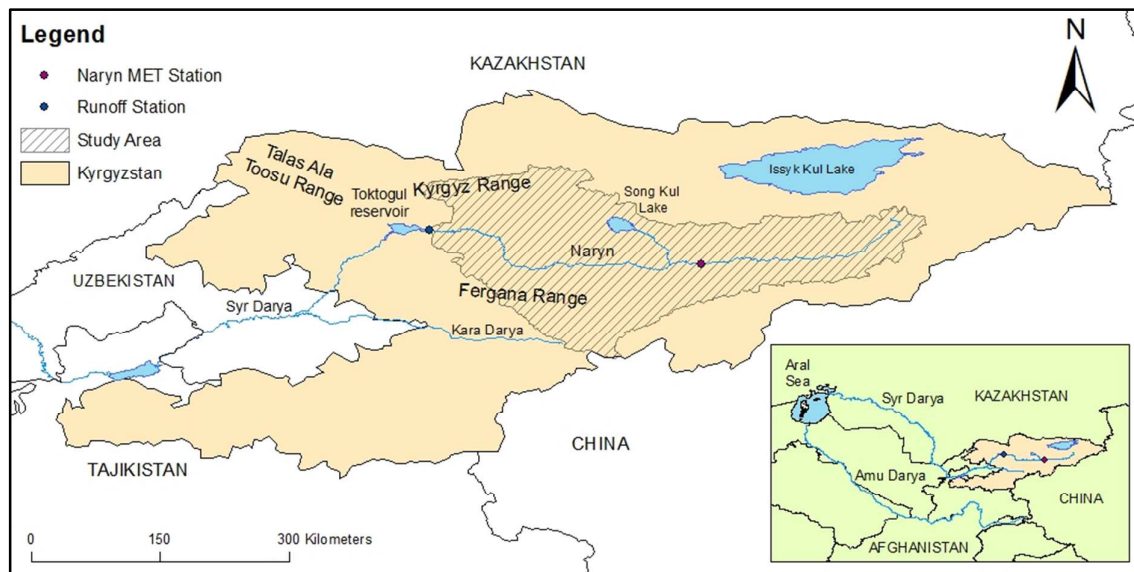
803

804 b)
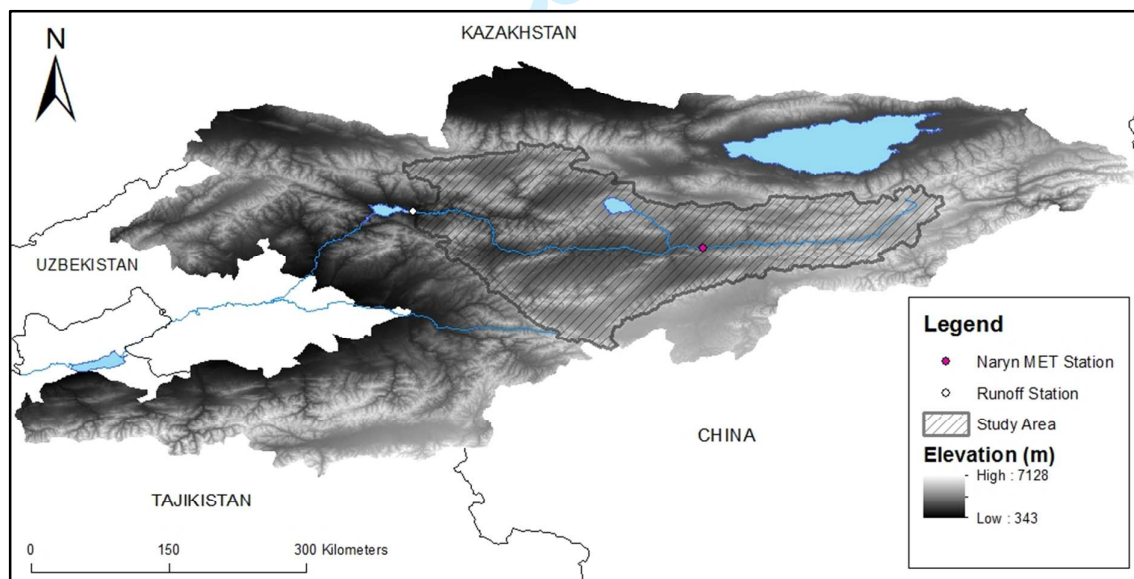
805

806

807

808

809

810   **Figure 2** Number of GPCC gauges used by TRMM across the study area for
811   selected years. The location of the gauge at Naryn is shown by the red point.

812
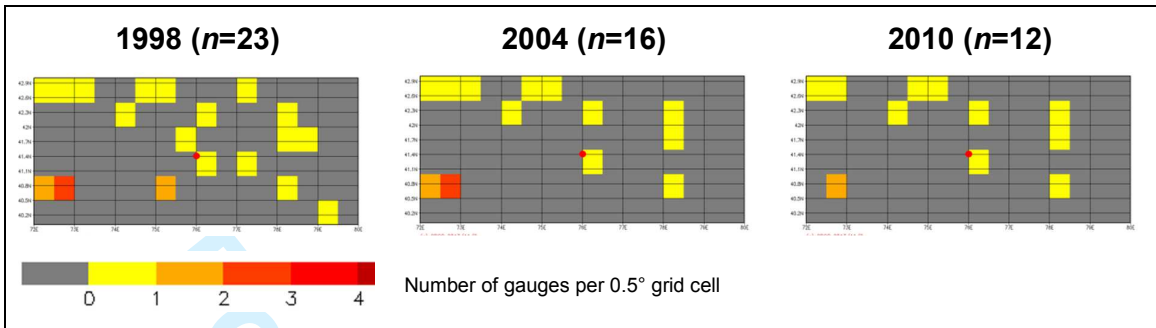
813   **Figure 3** Gauge versus 0.5° TRMM for a) monthly mean and b) annual precipitation
814   totals at Naryn 1998-2012.

815   a)
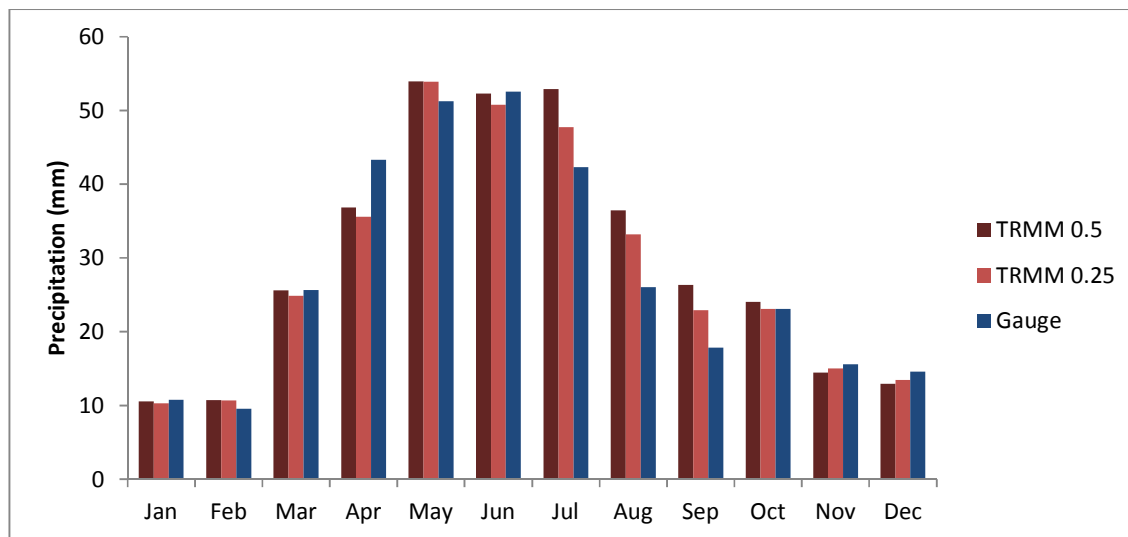
816

817   b)
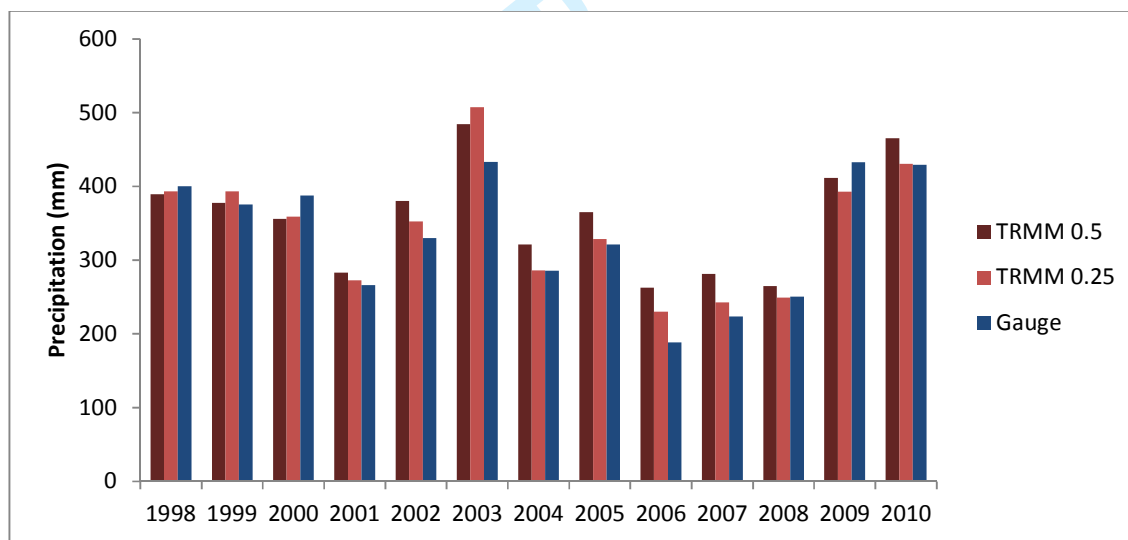
818

819

820   **Figure 4** Monthly total precipitation recorded by the gauge at Naryn compared with
821   the nearest a) 0.5° TRMM and b) 0.25° TRMM cell.

822   a)
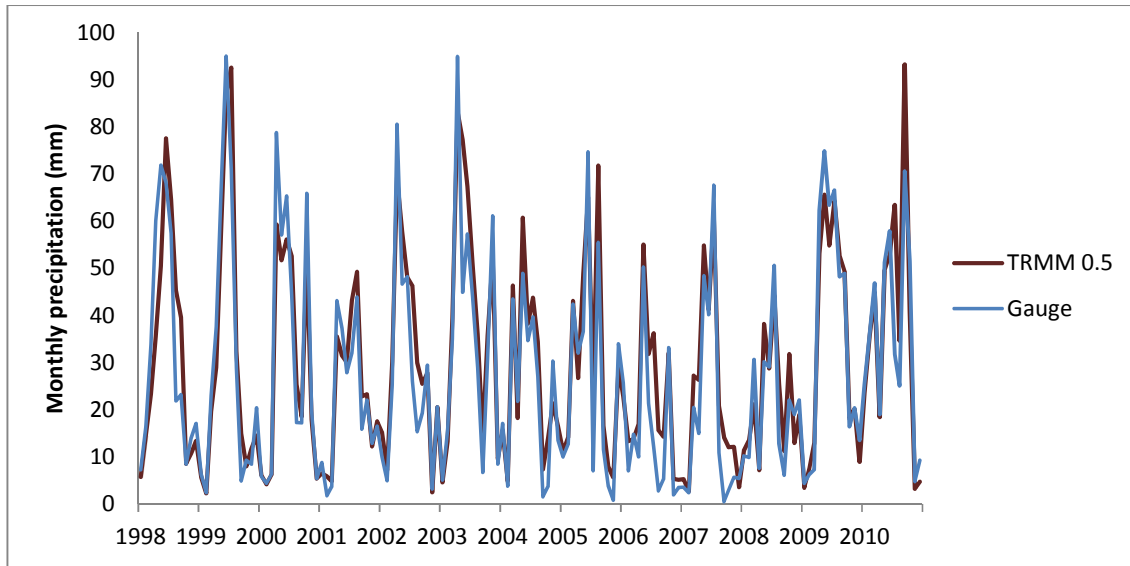
823

824

825   b)
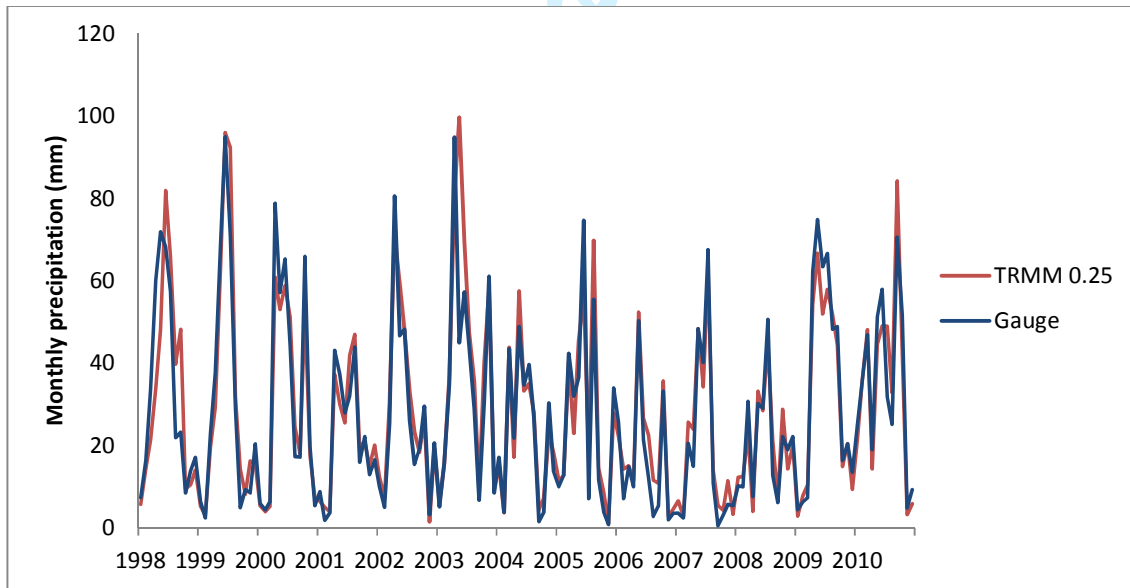
826
827

828   **Figure 5** Cumulative monthly precipitation totals for Naryn meteorological station,
829   coincident 0.5° TRMM and 0.25° TRMM cells 1998-2010.
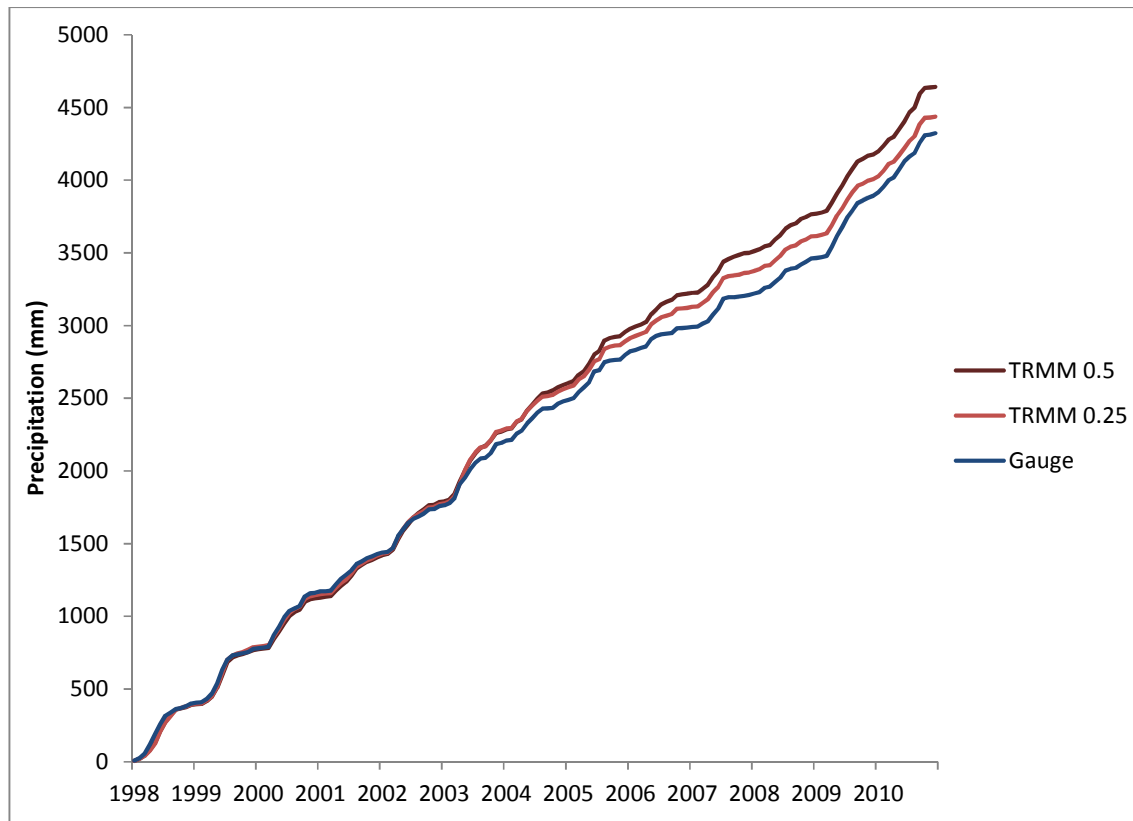
830
831
832
833
834
835

836   **Figure 6** Cumulative percentile distributions of gauged, 0.5° TRMM and 0.25° TRMM

837   daily precipitation amounts at Naryn 1998-2012.

838

839

840
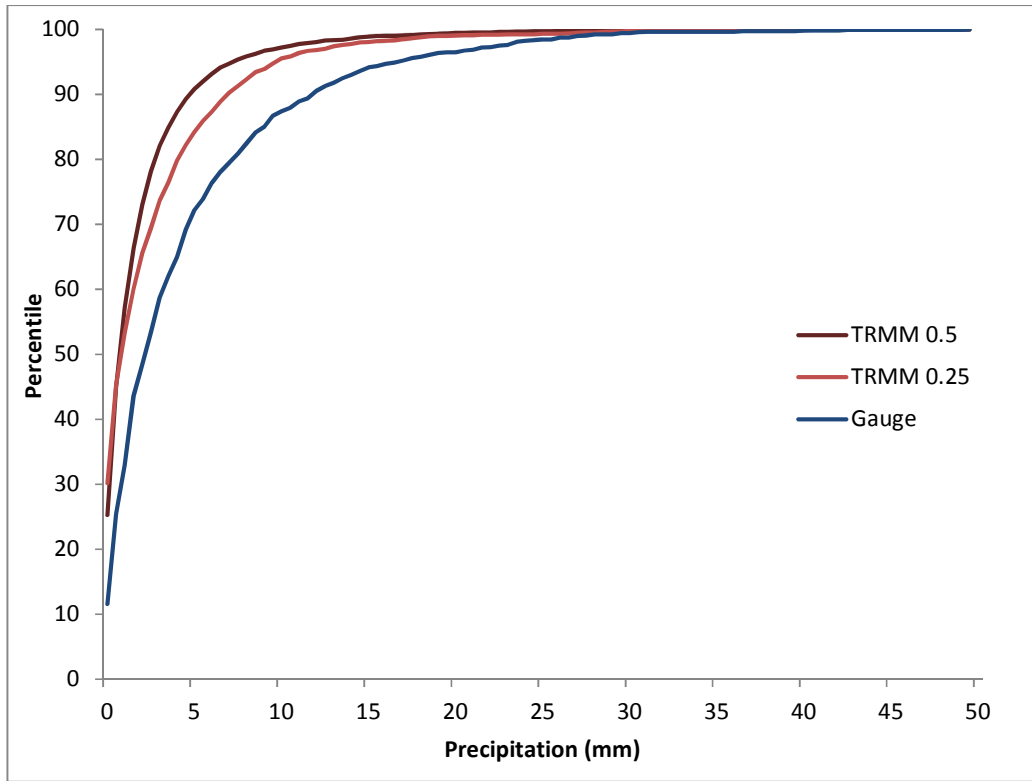
841   **Figure 7** Correlation between nearest 0.5° TRMM estimates and gauge a) daily and
842   b) monthly precipitation at Naryn 1998-2012

843   a)
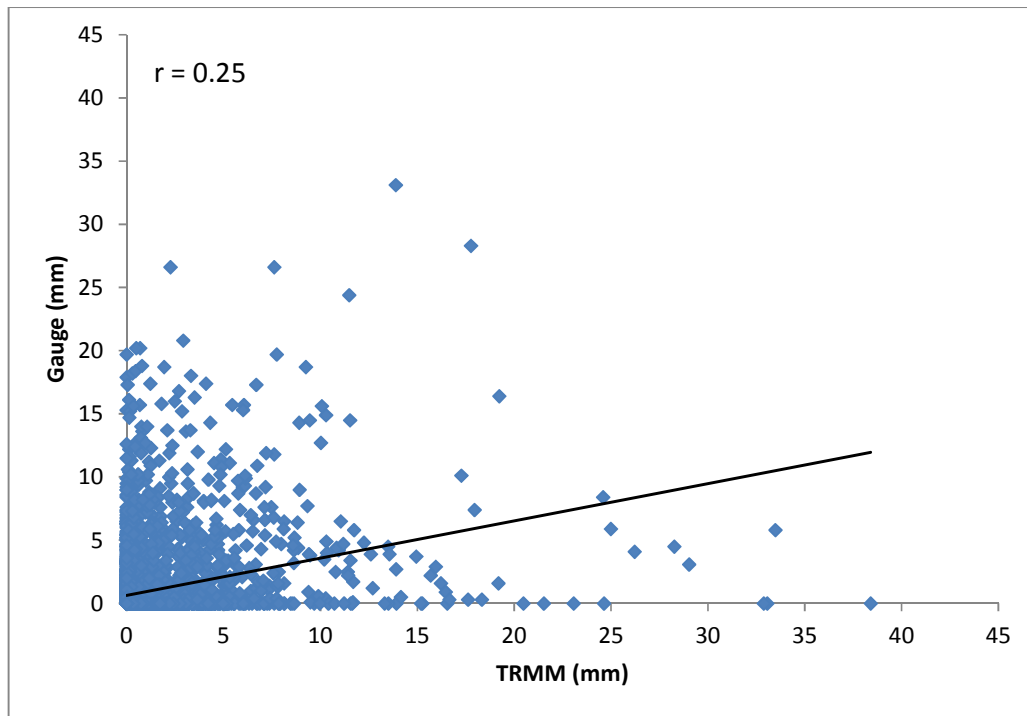
844

845   b)
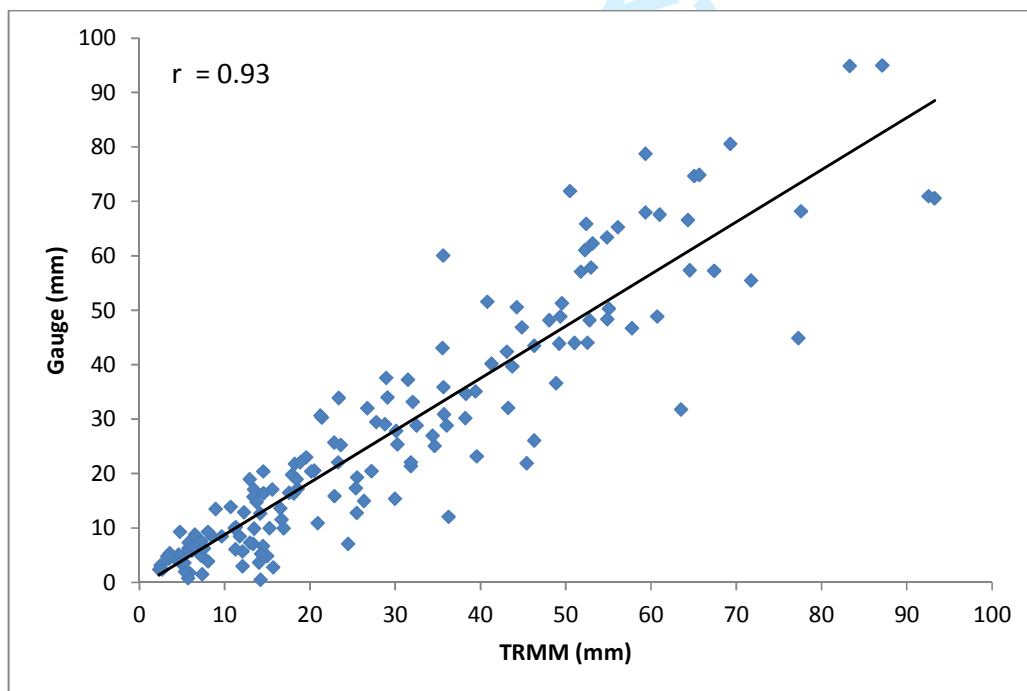
846

847

848   **Figure 8** Correlation between a) daily and b) monthly precipitation gauge at Naryn
849   and concurrent 0.5° TRMM estimates 1998-2012.

850   a)
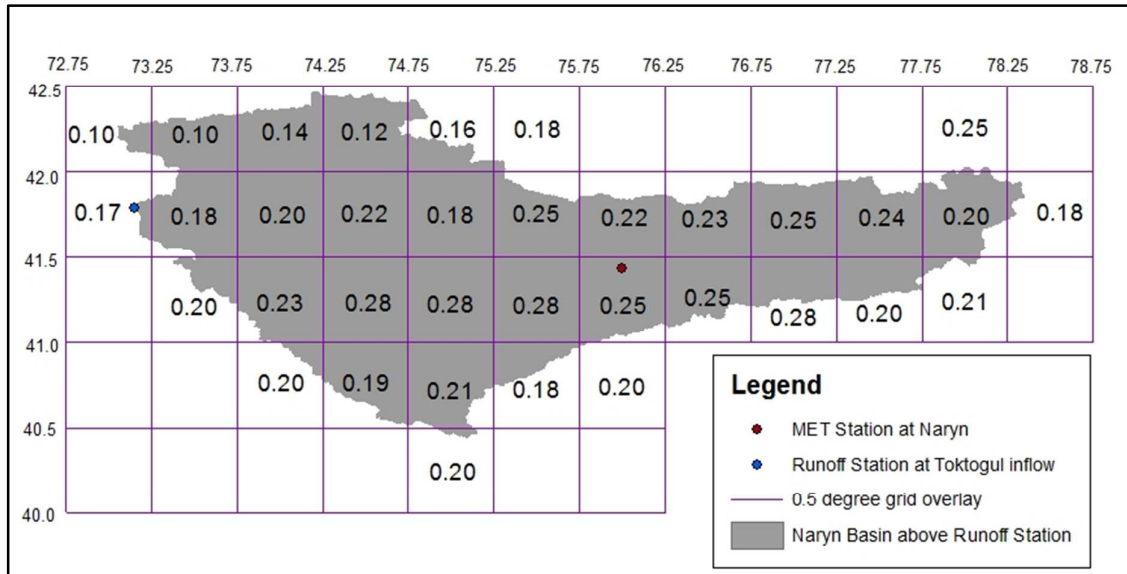
851

852   b)
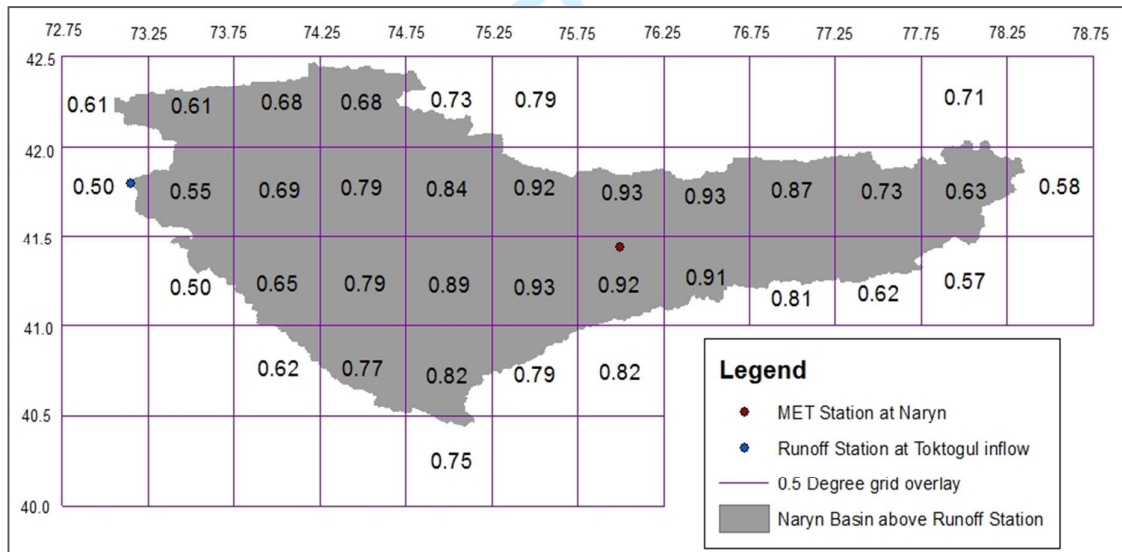
853
854

855

856   **Figure 9** Observed annual (upper panels) and monthly (lower panels) discharge into
857   Toktogul (left) and air temperature at Naryn (right).
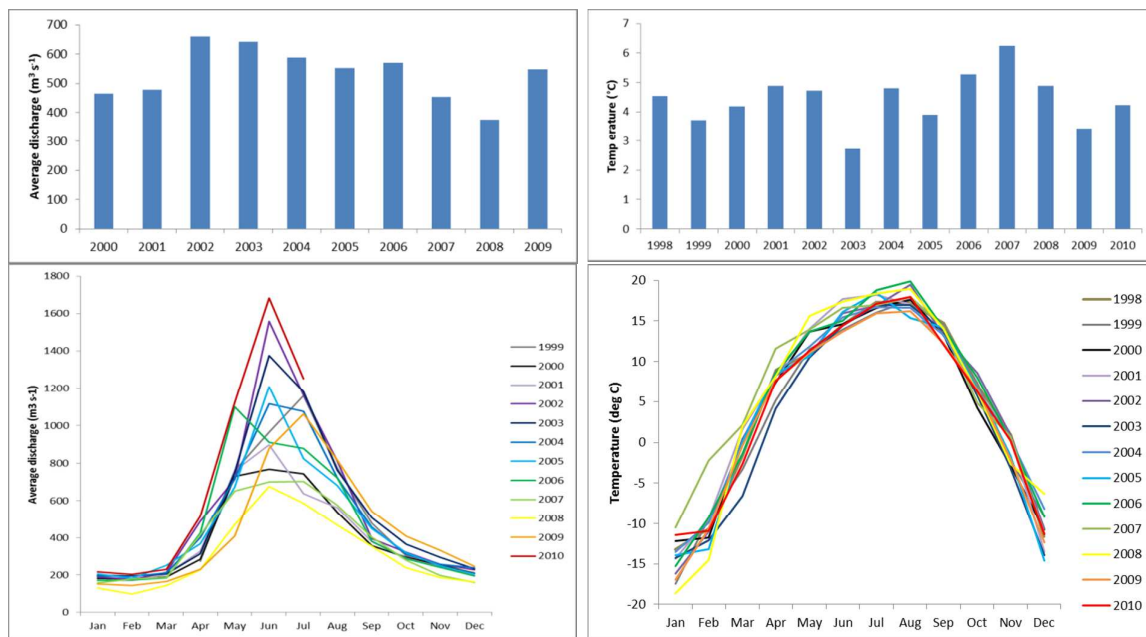
858

859

860

861

Figure 10 Amount of variance in gauged monthly discharge at Toktogul explained by 0.5° TRMM with lag=0 (upper left), lag=1 (upper right), lag=2 (lower left) and lag=3 (lower right) months for the period May 1999 to July 2010 inclusive
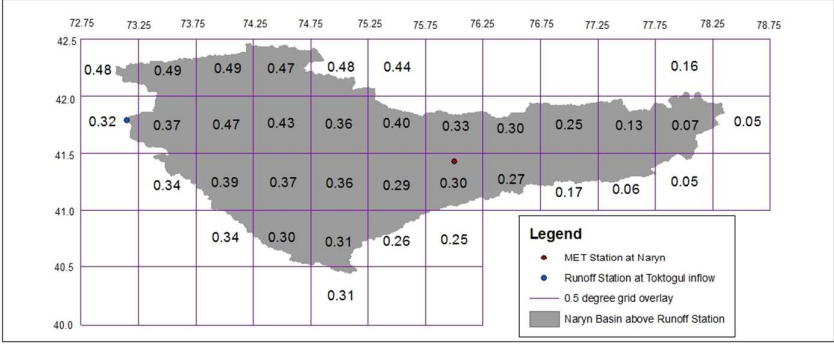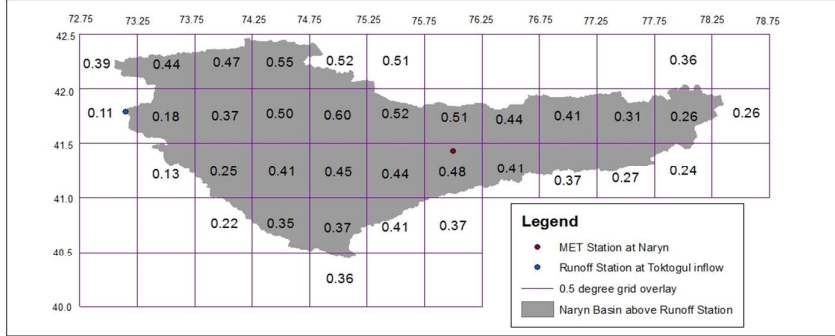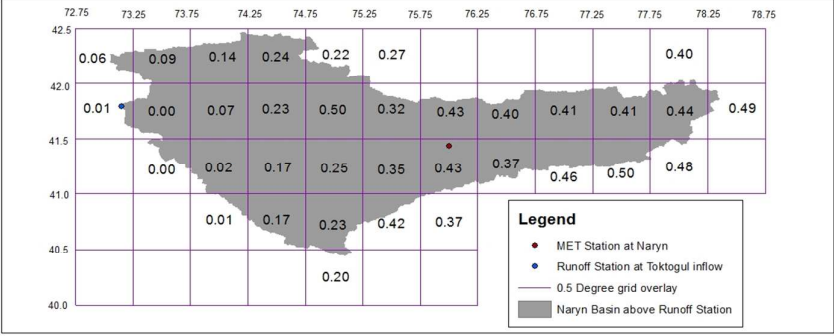

41
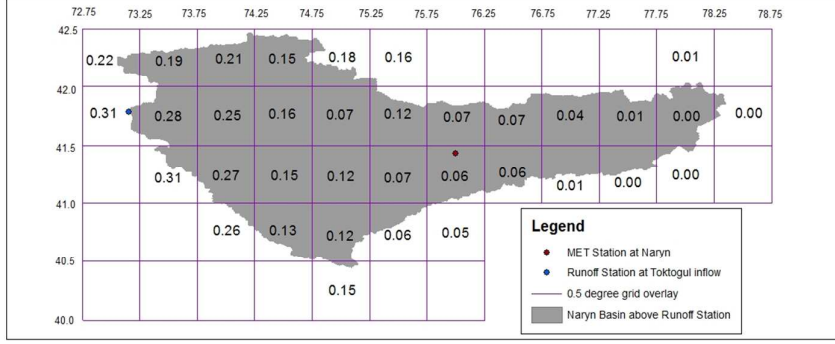
Figure 11 Correlation (*r*) of gauged flows with lagged predictors averaged over one to six months: temperature (T); precipitation measured at Naryn (PN); precipitation estimates from TRMM for the basin area (PA), and optimum location (PO). For *n*=130 and at p=0.05 significance level, r_{crit}=0.17.

1
2
3
4
5
6
7
8
9
10
11
12
13
14
15
16
17
18
19
20
21
22
23
24
25
26
27
28
29
30
31
32
33
34
35
36
37
38
39
40
41
42
43
44
45
46
47
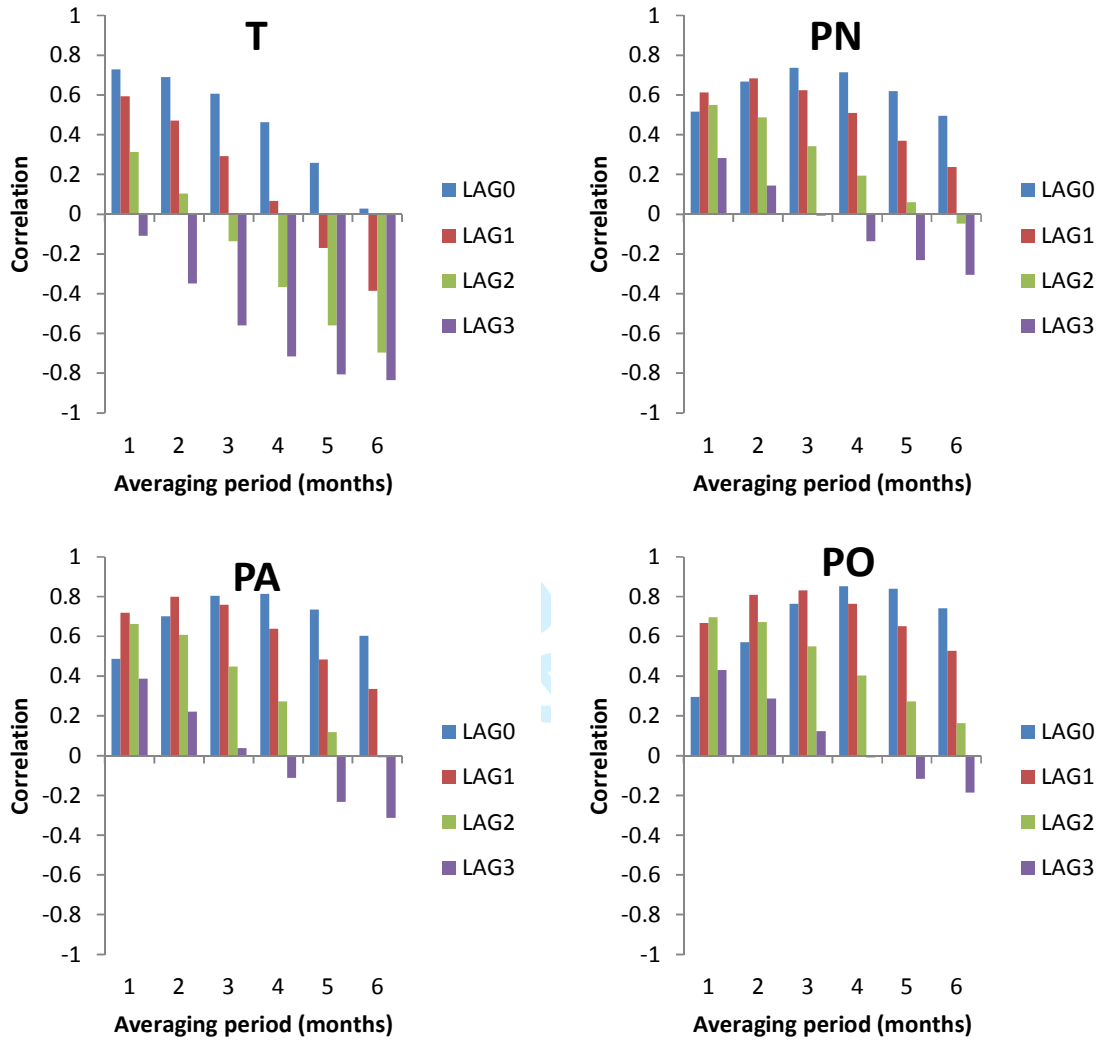48
49
50
51
52
53
54
55
56
57
58
59
60

Figure 12 Cross-validated model forecasts with lead-time one (Q1), two (Q2) and three (Q3) months compared with long-term monthly mean discharge (ZOF).
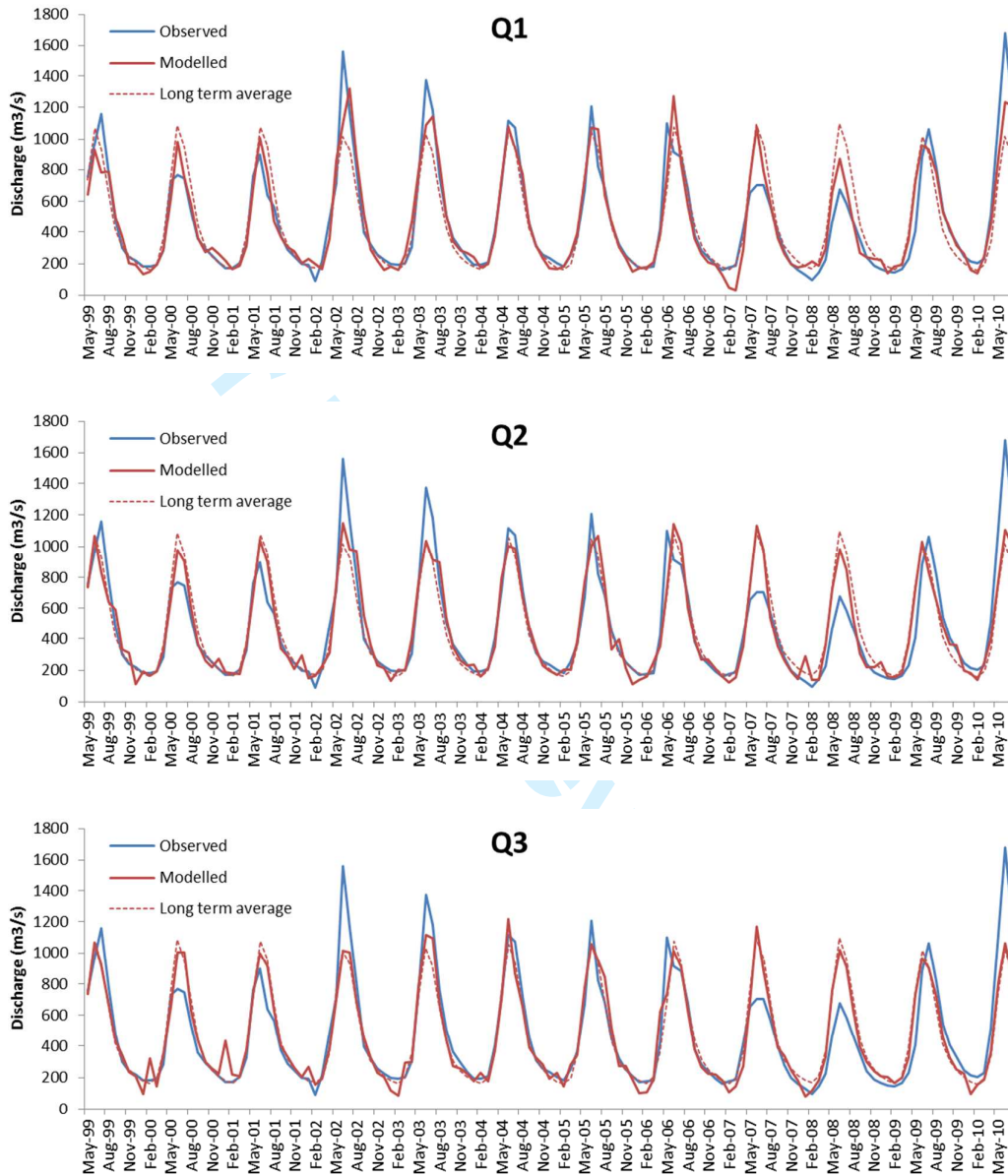

43

Figure 13 Daily precipitation and discharge series for the River Naryn during melt seasons with large residuals in the t+1 forecast (see Q1 in Fig.12).